Biological Effects of Millimeter-Wave Irradiation on Mice—Preliminary Results

A. Bellossi, G. Dubost, J. P. Moulinoux, M. Himdi, M. Ruelloux, and C. Rocher

***Abstract*—Millimeter waves at 60 GHz are suitable for discreet radio contact in a restricted area, especially for indoor high-rate communications. Such wave exposures have not been reported. That is the reason why a study of possible biological effects upon living beings was required. An experimental irradiation device was calibrated and used to irradiate mice. Specific absorption rate and internal fields have been computed for a mouse irradiated at 60 GHz. The measured power flux in free space at the irradiation area is close to 0.5 mW/cm^2, this probably produces some subtle biological effects. To look for possible biological effects, we exposed DBA2 mice grafted either with L1210 cells or with Lewis tumor cells and healthy Swiss mice. There were four obvious observations: there is an individual sensitiveness to 60 GHz waves; the survival of mice grafted with L1210 cells could be increased; the growth of Lewis tumor was enhanced; and the activity of Swiss mice was increased. In any way, those effects have to be taken into account, and we suggest prudence before using a 60-GHz wave for indoor communications.**

***Index Terms*—Biological effects of electromagnetic radiations.**

I. Introduction

THE selective absorption of millimeter waves in the atmosphere is chiefly due to both electronic transitions in the oxygen atom and pure rotational transitions in the water molecule. The microwave absorption of O_2 and H_2O has been investigated both experimentally and theoretically. Millimeter waves are attractive because of the small size of the antenna or wave collector used for a given directivity, and especially in case of discreet communications. From measured and calculated wave absorptions through the atmosphere and due to resonance phenomena, we have deduced the following.

- *Two frequency bands up to 45 GHz and between 75–115 GHz with a weak absorption (lower than 1 dB) due to oxygen and water vapor*. Civil and military applications are concerned with communications between satellites or missiles fitted with self-directional systems.
- *Three frequency windows with a strong absorption*. Two are related to oxygen at 60 and 120 GHz, and one with regard to water vapor at 190 GHz. These frequencies are suitable for discrete radio contact in a restricted area, especially at 60-GHz frequency for indoor high-rate communications, which are ongoing today. Extraterrestrial irradiation at 60 GHz is unknown in our environment due to the strong atmosphere absorption. That is why the study of possible biological effects upon living beings is required. Most studies related to the interactions between millimeter waves and living come from Russia and Eastern European countries. The Russian safety is stricter than that of most western countries, whose standards are only essentially based on the calculated thermal load that would be produced on people exposed to RF radiations, especially during experiments that are necessary to develop high-power military systems. In fact, it was important to discover the possible biological fields subtle effects.

Manuscript received November 12, 1999; revised May 3, 2000.

A. Bellossi, M. Ruelloux, and C. Rocher are with the Faculté de Médecine, Laboratoire Biophysique, University of Rennes I, 35042 Rennes, France.

G. Dubost and M. Himdi are with the Laboratoire Antennes et Réseaux, Unité Propre de Recherche de l'Enseignement Supérieur Associée au Centre National de la Recherche Scientifique 6075, University of Rennes I, 35042 Rennes, France.

J. P. Moulinoux is with the Faculté de Médecine, Laboratoire Génétique et Biologie Cellulaire, University of Rennes I, 35042 Rennes, France.

Publisher Item Identifier S 0018-9480(00)09703-9.

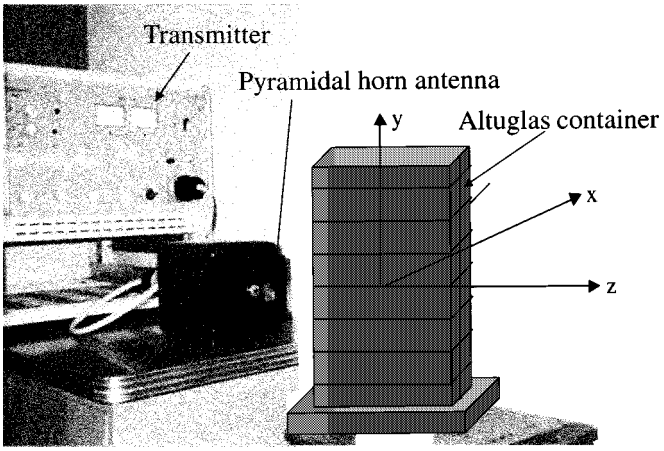

Fig. 1. Experimental irradiation device.

II. Experimental Irradiation DeviceRecall of Propagation in Lossy Dielectric Medium

In a first stage, the irradiation is supported by mice that are exposed to the radiation of an experimental device composed of a transmitter connected to a pyramidal horn antenna. This device has been courteously lent by Centre National d'études des Télécommunications (CNET), Lannion, France (Fig. 1). A detailed description of the mice restrainers is given in Section V.

A. Transmitter Calibration

The aim of the calibration procedure is to determine the power level radiated from the generator. The millimeter-wave generator (or transmitter) output is an opened rectangular waveguide of 3.76 mm $\times$ 1.88 mm section, which acts between 50–75 GHz. The input spectrum analyzer, used for the calibration, is an opened rectangular waveguide of 4.78 mm $\times$ 2.39 mm section, which acts between 40–60 GHz. At 60 GHz,

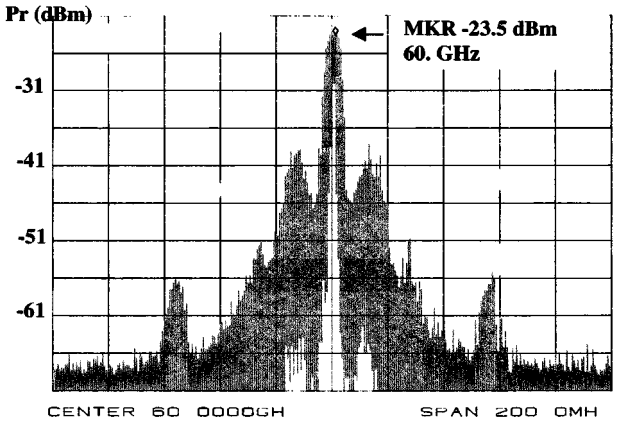

Fig. 2. Transmitter spectrum patterns around 60 GHz.

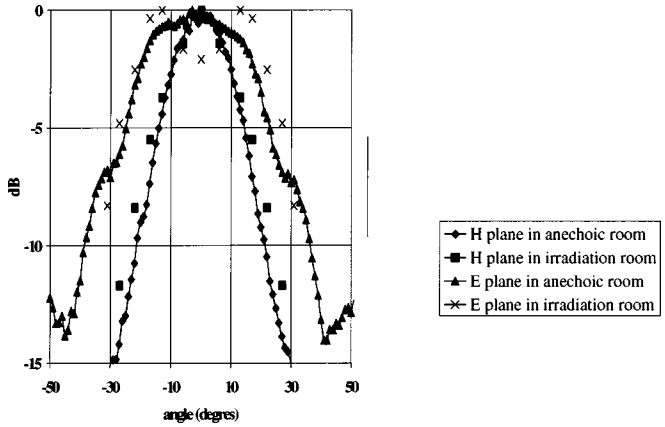

Fig. 3. Horn radiation patterns.

the linear isotropic gains of these two radiating apertures are $G_E = 3.55$ (5.5 dB) for the generator and $G_R = 5.74$ (7.6 dB) for the spectrum analyzer.

The distance between the two radiating aperture centers is equal to $d = 0.2$ m. The power measured by the spectrum analyzer in terms of frequency is shown in Fig. 2. At 60 GHz, the maximum is equal to -23.5 dBm, namely, $P_r = 4.4710^{-6}$ W.

From (1), we deduced the transmitted power P_E

$$P_E = P_r(4\pi d)^2/(G_E \cdot G_R \lambda^2). \quad (1)$$

With $\lambda = 5 \cdot 10^{-3}$ m, $P_E = 55$ mW. This value is identical with that given by the manufacturer.

B. Pyramidal Horn-Antenna Calibration

The rectangular radiation aperture of the horn antenna has a section of 22.2 mm $\times$ 16.7 mm. Its E-plane is the vertical plane related to the irradiation room and the H-plane is the horizontal plane. In an anechoïc room, we measured the radiation patterns, which are shown in Fig. 3. E- and H-planes are yoz and xoz (Fig. 1). The mice are distributed between the following two rows: 1) For six mice, the section of the six compartments is ± 43 mm in the E-plane and ± 29 mm in the H-plane. This corresponds to a variation of 1 dB in the E-plane and 2 dB in the H-plane (see Fig. 3). 2) For ten mice, the section is equal to ± 72 mm in the E-plane and ± 29 mm in the H-plane, and corresponds to a variation of 2.5 and 2 dB. This, we can consider that the field is equivalent in every compartments.

The maximum linear isotropic gain, which has been measured at 60 GHz, is equal to 47 (namely, 16.7 dB). The theoretical isotropic gain of a pyramidal horn is given by [1, p. 141]

$$G_M(\text{dB}) = 10.08 + 10\log 10(S/\lambda^2) - L_E - L_H. \quad (2)$$

Here, S is the aperture section (371 mm^2). The L_E and L_H factors, which account for the reduction in gain due to the phase error caused by the flare, are given in terms of horn longitudinal dimensions. With $L_E = 4$ dB and $L_H = 0.5$ dB, we find from (2) that $G_M = 17.3$ dB. The antenna gains deduced from experience and theory are very close.

C. Fields Radiated by the Device

We calculate the field radiated by the device at a point located on the pyramidal horn axis. At a distance r higher than the Fraunhofer zone, the electric field is equal to

$$|E| = (1/r)\sqrt{60 P_E G_M}. \quad (3)$$

With $r = 0.2$ m, $P_E = 55 \cdot 10^{-3}$ W, $G_M = 47$, we deduced $|\vec{E}| = 62$ V/m crest and $|\vec{H}| = 0.16$ A/m crest, and the power flux density $\Phi = 0.51$ mW/cm^2. This density has been measured several times by means of a detector during the experiments. By considering only thermal effects, the RF exposure limits at 60 GHz for various standards is between 0.2–5 mW/cm^2 [2].

D. Electromagnetic Plane Wave Falling Upon Isotropic Lossy Dielectric Medium

The relative permittivity, respectively, conductivity, of the three-dimensional medium is εr, respectively, σ. For a normal incidence, the percentage of transmitted power is given by [3, p. 62]

$$\tau = 1 - |\Gamma_r|^2 \quad (4)$$

where

$$\Gamma_r = \sqrt{u} - 1/\sqrt{u} + 1 \quad (5)$$

is the reflection coefficient of the electric field with

$$u = \varepsilon_r(1 - j\sigma/\omega\varepsilon_r\varepsilon_o). \quad (6)$$

The wave impedance of the medium is

$$Z_m = \sqrt{\mu_o/u\varepsilon_o}. \quad (7)$$

The refraction coefficient of electric field is equal to

$$\Gamma_t = 2/(1 + \sqrt{u}). \quad (8)$$

The attenuation of the electromagnetic fields inside the medium is in the form

$$\exp(-z/\delta) \quad (9)$$

TABLE I

Organ	Breast Fat	White matter	Bladder	Lung inflated	Skin	Liver	Grey matter
σ (S/m)	1.5	9	5.5	8.5	15	15	20
ε_r	3.5	25	9	10	25	20	35
τ (4)	0.89	0.54	0.71	0.66	0.52	0.54	0.46
δ(mm) (10)	6.7	3.0	3.0	2.1	1.85	1.7	1.6
$\|\Gamma_t\|$ (8)	0.68	0.33	0.48	0.44	0.32	0.34	0.28
Z_m(ohm) (7)	198+j37	73+j11	114+j29	101+j34	69+j18	73+j22	58+j14

Organ	Bone cancellous	Blood Spleen Muscle Cervix	Ovary Aorta	Heart Kidney	Uterus Thyroid	Testes
σ(S/m)	15	25	20	25	30	35
ε_r	15	30	20	25	30	35
τ (4)	0.57	0.46	0.52	0.48	0.45	42
δ(mm) (10)	1.5	1.3	1.3	1.15	1.05	1.0
$\|\Gamma_t\|$ (8)	0.37	0.28	0.33	0.30	0.27	.26
Z_m(ohm) (7)	78+j30	58+j20	68+j26	61+j23	55+j21	51+j20

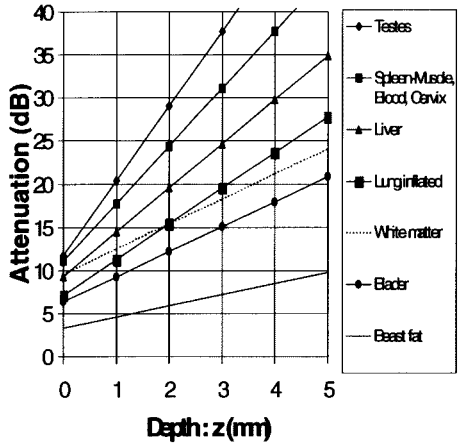

Fig. 4. Attenuation in some living organs at 20 GHz.

where δ is the penetration depth given by [3, p. 39]

$$\delta = \frac{\lambda_o}{2\pi}\left[\frac{-\varepsilon_r}{2} + \frac{1}{2}\sqrt{\varepsilon_r^2 + \frac{\sigma^2}{\omega^2\varepsilon_o^2}}\right]^{-1/2} \tag{10}$$

where λ_o is the free medium wavelength.

III. Penetration of Millimeter Waves Inside Some Living Organs at 20 GHz

Next, Table I shows, for some living organs, the relative permittivity ε_r and conductivity σ measured at 20 GHz, which is the highest available frequency published and given by [4]. We deduced, from (4) and (10), the transmitted power τ and the penetration depth δ.

In this table, the classification has been done by following a decreasing order for the penetration depth δ. It appears that the millimeter-wave penetration is easier for breast fat because of both the highest penetration depth ($\delta = 6.7$ mm) and the strongest transmitted power ($\tau = 0.89$). This attenuation is equal to

$$\begin{aligned} A(dB) &= -20\log_{10}|\Gamma_i| + 8.69z/\delta \\ &= -20\log_{10}|E_i/E|. \end{aligned} \tag{11}$$

$|\Gamma_\tau|$ and δ are specified in Table I and z is the distance from the medium surface. This is shown in Fig. 4 for some living organs.

IV. Average Specific Absorption Rate and Internal Field for a Mouse Irradiated at 60 GHz

In that paragraph, we demonstrate that the internal field, radiated by means of our device, inside a mouse, may produce only subtle biological effects (no thermal effect). The normalized average specific absorption rate $(\mathrm{SAR})_N$ related to a plane wave at 60 GHz applied to a mouse for a vertical polarization is given in [5].

It is equal to $(\mathrm{SAR})_N = 0.6$ W/kg per mW/cm^2. With our device, we operate at a distance $r = 0.2$ m where $\Phi = 0.51$ mW/cm^2 (see Section II-C). The SAR is then equal to $(\mathrm{SAR}) = 0.6 \times 0.51 = 0.31$ W/kg. The average internal field is given by

$$|E_i|_a = \sqrt{\rho_m(\mathrm{SAR})/\sigma_m} \tag{12}$$

where σ_m is the average body conductivity and ρ_m is the average tissue density. With $1 < \sigma_m < 35$ S/m and $\rho_m = 10^3$ kg/m^3, we find: $3 < |E_i| < 18$ V/m.

The potential magnitude $|V_m|$, which appears within the outside spherical cell of radius R and thickness Δ belonging to a specific organ and illuminated by an internal electric field $|E_i|$, is given by [6]

$$|V_m| = \Delta|E_m| \tag{13}$$

$$|E_m| = \frac{1,5|E_i|}{\Delta}\cdot R. \tag{14}$$

For example, with $R = 100\,\mu$m, $\Delta = 10$ nm, we have obtained from (13) and (14): $4.5\ 10^4 < |E_m| < 2.7\ 10^5$ V/m and $0.45 < V_m < 2.7$ mV. The electric field $|E_m|$ across the membrane has no effect upon the ion agility, especially for the elongation [6], which is given by

$$|\vec{s}| = q/m \cdot (|E_m|/\omega^2). \tag{15}$$

In effect, for instance with H^+, which has $q/m = 9.6 \cdot 10^7$C $\cdot$ kg^{-1}, we obtain from (15) with $|E_m| = 2.7 \cdot 10^5$ V/m: $|\vec{s}| = 0.2$ nm.

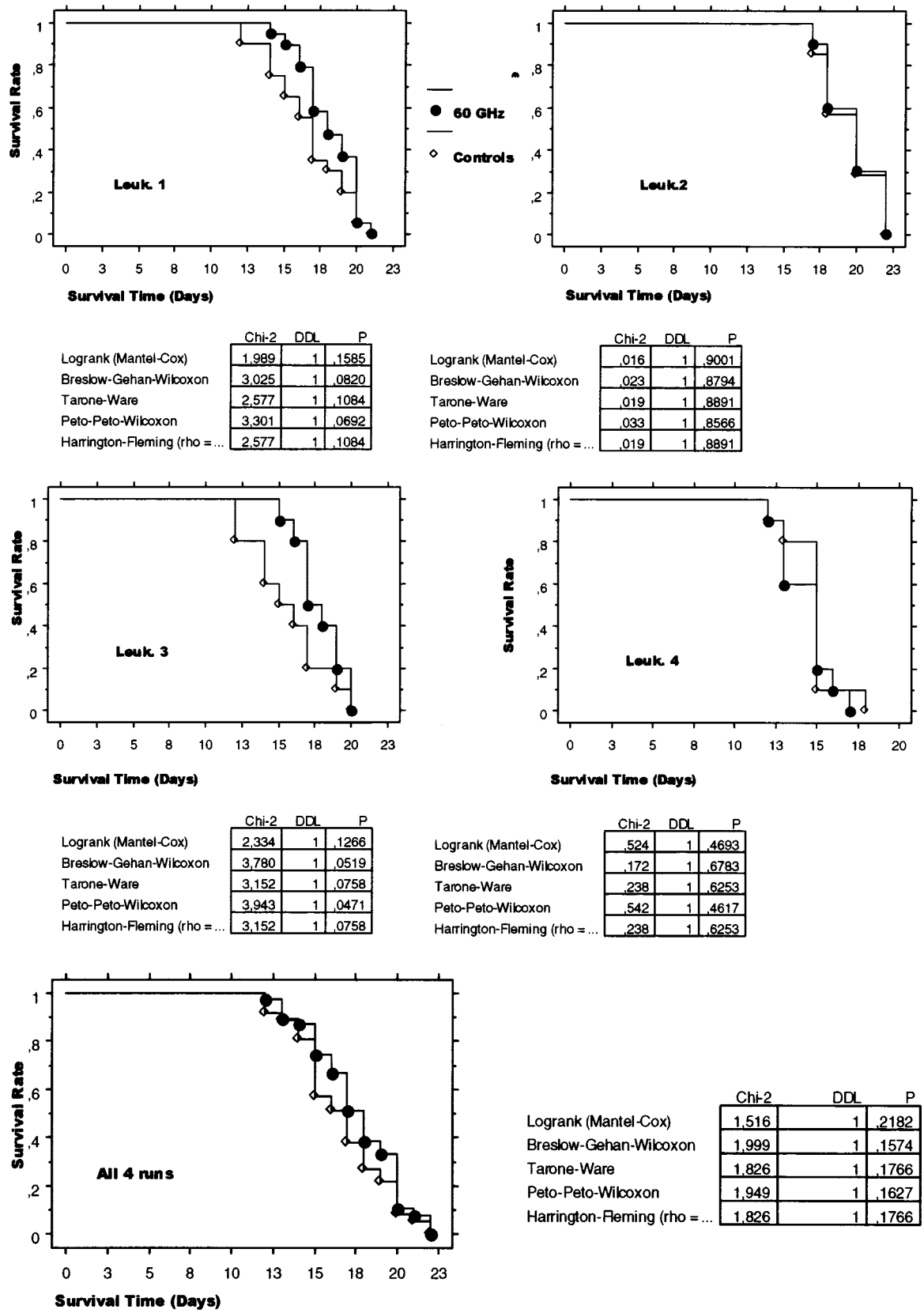

	Chi-2	DDL	P
Logrank (Mantel-Cox)	1,989	1	,1585
Breslow-Gehan-Wilcoxon	3,025	1	,0820
Tarone-Ware	2,577	1	,1084
Peto-Peto-Wilcoxon	3,301	1	,0692
Harrington-Fleming (rho = ...	2,577	1	,1084

	Chi-2	DDL	P
Logrank (Mantel-Cox)	,016	1	,9001
Breslow-Gehan-Wilcoxon	,023	1	,8794
Tarone-Ware	,019	1	,8891
Peto-Peto-Wilcoxon	,033	1	,8566
Harrington-Fleming (rho = ...	,019	1	,8891

	Chi-2	DDL	P
Logrank (Mantel-Cox)	2,334	1	,1266
Breslow-Gehan-Wilcoxon	3,780	1	,0519
Tarone-Ware	3,152	1	,0758
Peto-Peto-Wilcoxon	3,943	1	,0471
Harrington-Fleming (rho = ...	3,152	1	,0758

	Chi-2	DDL	P
Logrank (Mantel-Cox)	,524	1	,4693
Breslow-Gehan-Wilcoxon	,172	1	,6783
Tarone-Ware	,238	1	,6253
Peto-Peto-Wilcoxon	,542	1	,4617
Harrington-Fleming (rho = ...	,238	1	,6253

	Chi-2	DDL	P
Logrank (Mantel-Cox)	1,516	1	,2182
Breslow-Gehan-Wilcoxon	1,999	1	,1574
Tarone-Ware	1,826	1	,1766
Peto-Peto-Wilcoxon	1,949	1	,1627
Harrington-Fleming (rho = ...	1,826	1	,1766

Fig. 5. Leukemia: survival curves.

Nevertheless, and without frequency precision, it appears that if cell membrane destruction is obtained for $100 < V_m < 300$ mV, subtle biological effects may be achieved for: 0.1 mV $< V_m < 1$ mV: [5]. We are in that situation.

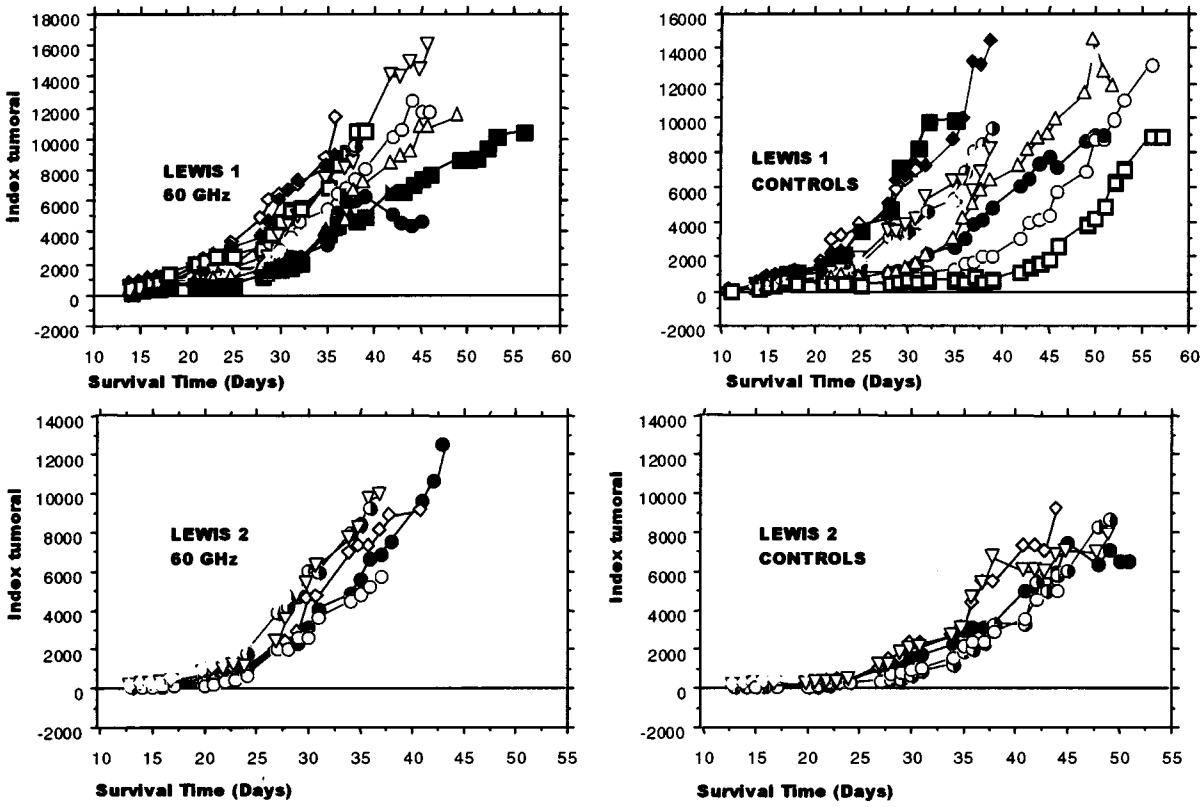

Fig. 6. Experiments with 10^6 Lewis grafted cells: tumoral indexes. Each curve represents the tumor in a mouse.

V. Exposure of Mice

A. Material and Methods

To our knowledge, biological effects due to a 60-GHz wave exposure have not been reported. To look for a possible effect on a living system, six-week-old DBA2 and Swiss female mice were used. For the exposure, a parallelepiped altuglas container measuring $68 \times 114 \times 298$ mm was divided into two rows of $29 \times 29 \times 100$ mm compartments (Fig. 1). Each compartment contained one mouse. The same mouse was always put into the same compartment. The center of the central compartments was placed at 20 cm from and on the axis of the radiating horn. The exposure took place five consecutive days a week until death. Each session lasted 30 min. During the time of exposure, the controls were into a container located far from the 60-GHz generator. The mice were weighed on each day of exposure.

DBA2 mice were grafted either with 20 000 L1210 leukemia cells by intraperitoneal injections or with Lewis tumor cells by intramuscular injection into the right rear legs; as soon as possible, the tumors were measured according three orthogonal diameters and a tumoral index was computed. For each experiment, 20 mice were used: ten controls and ten exposed mice. Four series received L1210 cells. Three series received Lewis tumor cells, two series 10^6 cells for a mouse, and one series 500 000 cells. At death, the brains, lungs, hearts, livers, spleens, kidneys, and tumors were weighed. Twelve healthy Swiss female mice (six controls and six exposed ones) were used. Their exposure took place at 10 A.M. Their individual activity was estimated for a 30-min-stay into an actimeter (OSYS, Laval, France) at 9 A.M, 23 h after the exposure. Moreover, the weight of food eaten was measured once a week.

B. Results

1) L1210 cells: Neither the growing curves nor the mean weights of the organs were significant of the effect. The survival curves of the controls and the exposed mice showed no difference in two series (average survival times with standard deviations in days of the controls and of the exposed mice: 19.6 ± 2 and 19.7 ± 1.9 for the second series, 14.8 ± 1.5 and 14.4 ± 1.6 for the fourth series). In the two other series, the exposure led to a benefit in the survival times (Fig. 5); the mean survival times were, respectively, 17.7 ± 2.3 and 19.1 ± 3 days, 15.6 ± 2.7 and 17.8 ± 1.7 days; a gain of two days with such an aggressive leukemia is worth attention.

An overall statistical test covering the data for all four runs was not significant, the average survival times with standard deviations for the controls and for the exposed mice being 16.7 ± 2.8 and 17.6 ± 2.7 days, respectively.

2) Lewis tumor: A 500 000 cell graft did not show noticeable difference, neither in the growing of tumors according to the tumoral indexes, nor in the average survival times (controls: 32.3 ± 5.5 days, exposed mice: 36.6 ± 3.10 days). On the other hand, the 10^6 cell grafts showed interesting effects; in the first experiment, the tumoral growths were more synchronous when the mice were exposed and more scattered in the controls (Fig. 6). The translation of that synchronism was revealed by a delayed death of some control mice, which is perceptible

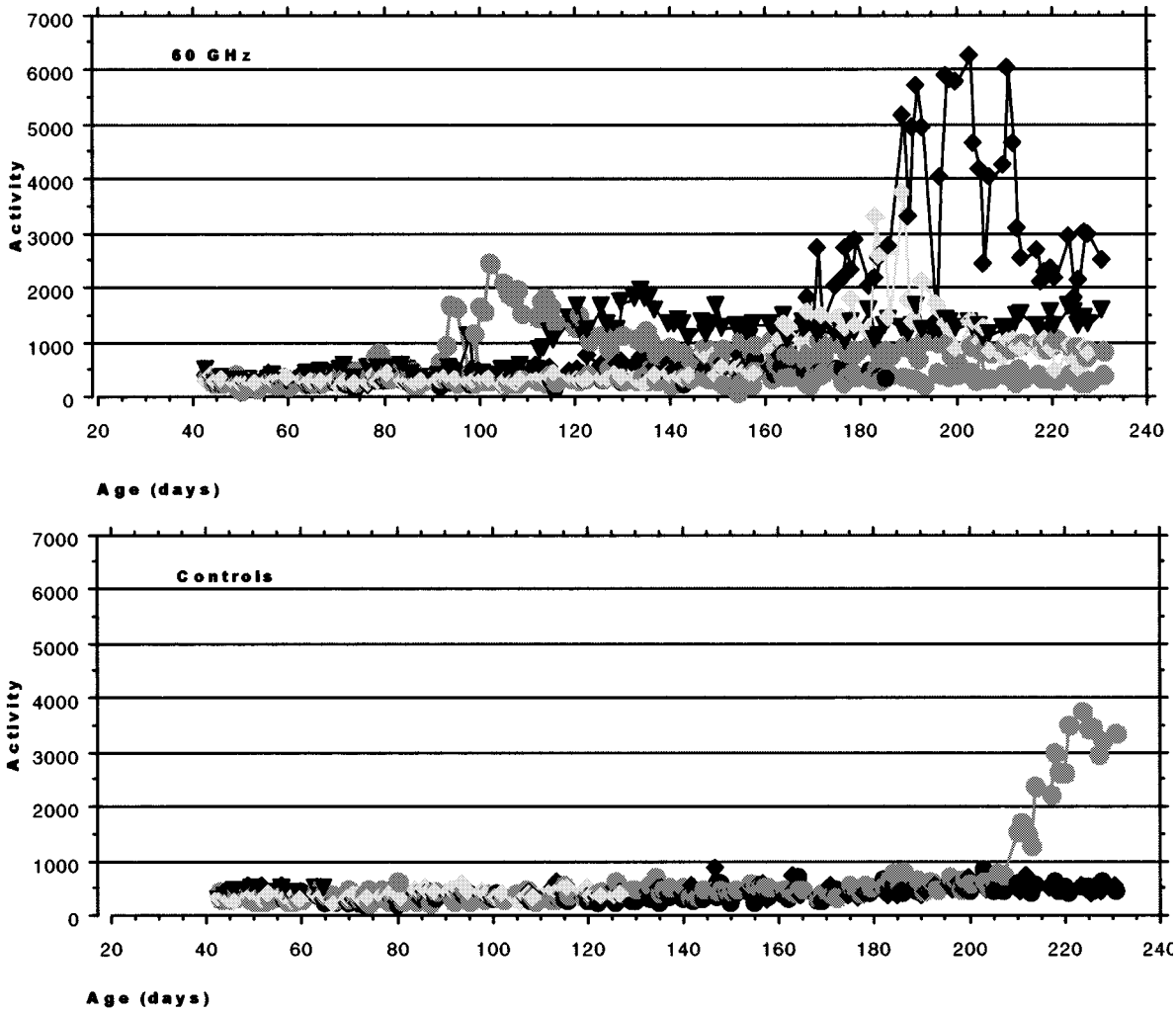

Fig. 7. Activity of Swiss female mice (each curve represents the activity of a mouse).

through the standard deviations of the survival times (controls: 46.4±9.1 days, exposed mice: 44.6±6.2 days).

3) Swiss mice: Those mice now have 231 days of age and the experiment is ongoing. Three control mice are dead and one exposed mouse have been accidentally killed. The following two facts are interesting: 1) the exposure does not change the growing curves and 2) in a previous experiment, the activity of two series of six Swiss female mice have been following from 40 days of age to more than 400 days of age. With the counting system of the actimeter, the activity measured for 30 min generally ranged between 50–500. In the present experiment (Fig. 7), a control mouse showed an increased activity from the 210th day of age, and reached a value of 3747. However, in the exposed group, four mice had an increased activity, which began at the 94th, 115th, 163rd, and 168th day of age and quickly reached 2428, 1920, 3709 and 6247, respectively. The activities progressively decreased and then became steady between 1000–1500. That increase of food consumption for the 180th day went with the increased activity (Fig. 8).

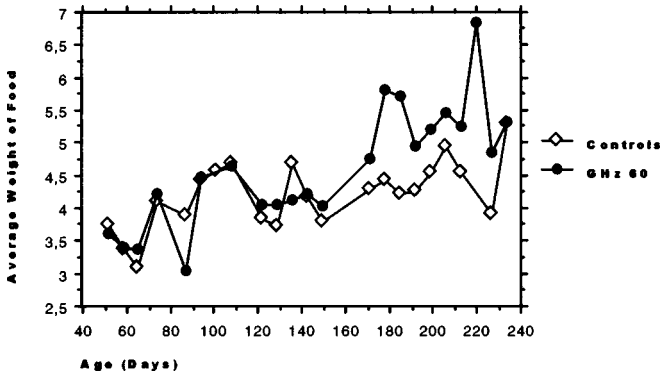

Fig. 8. Swiss mice: average weight of food a day for a mouse.

C. Discussion

At this time, three effects can be noted: 1) a trend to a longer survival time of the mice grafted with L1210 cells, for two series out of four; 2) a synchronization with a possible faster growth of Lewis tumors; and 3) an increase activity of some Swiss healthy mice.

Synchronization of Lewis tumor growth may be due to an effect either on the tumor cells, or to an efficient decrease of the immune system, or both. A deleterious effect of the 60-GHz radiation on the either normal or abnormal leucocytes could explain a possible gain in the survival times of L1210 grafted mice and a shortage in the immune system of Lewis grafted mice.

The sudden increase in activity may be considered as a rare, but normal, occurrence since it appeared in a control mouse. It appeared in the central nervous system like a hit target giving rise to the release of a neurotransmitter from the stock area. The emptying of those stocks would lead to a lesser activity, however, greater than in a nonexposed state, due to the immediate use of the synthesized drug. Moreover, that activity happened at different times for the different mice, which is in favor of individual sensitiveness to the 60-GHz radiation.

VI. Conclusion

On one hand, these first results need to be confirmed about either a direct or an indirect effect on promotion of malignant tumors. On the other hand, it will be interesting to see if the increase in activity will go with an effect on the life span. In any way, they warrant prudence before using a 60-GHz wave for indoor communications.

References

[1] G. Dubost and S. Zisler, *Antennes à Large Bande. Théorie et Applications*. Masson Paris, France: Masson, 1976, p. 337.
[2] E. Karabetsos *et al.*, "Documents regarding the sage exposure of humans to electromagnetic fields," European Community, Cost 244, 1984.
[3] G. Dubost, *Propagation Libre et Guidée des Ondes Électromagnétiques: Applications aux Guides et Fibers Optiques*. Masson Paris, France: Masson, 1995, p. 291.
[4] C. Gabriel and S. Gabriel, "Dielectric properties of body tissues," King's College, London, U.K., June 1996.
[5] *Radiofrequency Radiation Dosimetry Handbook*, U.S. Air Force School of Aerospace Med., Brooks AFB, TX, 1997.
[6] G. Dubost, A. Bellossi, M. Himdi, and J. P. Daniel, "Safety irradiation of humans by R. F. near fields due to dipoles," in *JINA'98*, Nice, Italy, pp. 639–642.

A. Bellossi, photograph and biography not available at time of publication.

G. Dubost, photograph and biography not available at time of publication.

J. P. Moulinoux, photograph and biography not available at time of publication.

M. Himdi, photograph and biography not available at time of publication.

M. Ruelloux, photograph and biography not available at time of publication.

C. Rocher, photograph and biography not available at time of publication.